

Informational entropy thresholds as a physical mechanism to explain power-law time distributions in sequential decision-making

Javier Cristín, Viçenc Méndez and Daniel Campos

(Dated: January 4, 2022)

While frameworks based on physical grounds (like the Drift-Diffusion Model) have been exhaustively used in psychology and neuroscience to describe perceptual decision-making in humans, analogous approaches for more complex situations like sequential (tree-like) decision making are still absent. For such scenarios, which involve a reflective prospection of future options to reach a decision, we offer a plausible mechanism based on the internal computation of the Shannon's entropy for the different options available to the subjects. When a threshold in the entropy is reached this will trigger the decision, which means that the amount of information that has been gathered through sensory evidence is enough to assess the options accurately. Experimental evidence in favour of this mechanism is provided by exploring human performances during navigation through a maze on the computer screen monitored with the help of eye-trackers. In particular, our analysis allows us to prove that: (i) prospection is effectively being used by humans during such navigation tasks, and a quantification of the level of prospection used is attainable, (ii) the distribution of decision times during the task exhibits power-law tails, a feature that our entropy-based mechanism is able to explain, in contrast to classical decision-making frameworks.

I. INTRODUCTION

In our daily life, we constantly find ourselves in situations that imply making decisions: what I am going to eat, which film I will see or if I am on time for the next bus. In all these situations we need to evaluate the different options available as a way to elucidate the best one. While exploring such situations would lie within the field of psychology, in the recent years there has been a growing interdisciplinary interest in decision-making. Determining the neural correlates of decision mechanisms constitute an important subject in cognitive and behavioral neuroscience [1–4]. Also, the mathematical study of decision strategies and its comparison to the subjects performance represents an important subject in game theory and econophysics [5, 6]. Last but not least, ideas from statistical physics and/or complex systems have also made its way; while most contributions to date focus on decision-making at the level of groups or collectives (see [7–11] for some reviews), tentative works suggesting physical principles that could be involved in individual decisions do also exist [12–16].

Up until now, large efforts have been put in understanding the dynamics and the characteristics of perceptual decisions, it is, those where sensory information provides direct evidence for choosing between the options available, as in the famous random dot motion task [17, 18]. As a result, a correspondence between such sensory information and the neuronal responses responsible for the evidence accumulation in the brain are assumed to be identifiable somehow. Alternatively, value-based or preferential decision-making (though the exact definition changes from one specific field to another) involves situations where a deliberative and subjective (up to some level) process is necessary to reach the decision, as for example when a subject is asked to choose between two food items. In such cases neural correlates become obviously more difficult to identify.

We can still introduce a third class of situations in which an objective answer to the task does exist but such an answer cannot be reached instantaneously from sensory information, because successive coupled decisions are involved. Following some existing literature (see, e.g., [19, 20] and references there in), we will denote these situations as *sequential* decision-making. Since these obviously require a higher cognitive capacity and a more reflective response by the subject in order to process the information, these situations are essentially restricted to humans (or maybe some other higher organisms). They include tasks like playing board games as chess, or solving mazes or tasks presented in some intelligence tests. All these examples involve decisions where a tree-like structure of future possibilities must be ideally built. So that, in the present work we will use the term *prospection* to denote such hypothetical, or mental, simulations of future events requiring high memory and abstraction capacities [21–23].

For the simpler case of perceptual decision-making, most theoretical frameworks aimed to explain their underlying mechanisms and dynamics lie within the so-called *accumulator* framework. In it, cognitive evidence (described through some effective stochastic process) is gained throughout the time until it reaches a given threshold, which then triggers the decision. The paradigmatic example is the Drift-Diffusion model (DDM) [24], where the relative evidence in favour of the different options is assumed to follow a Brownian diffusion process (which introduces cognitive fluctuations or noise in the process), with a drift that accounts for the trend towards the correct option. Nowadays, it is widely accepted among psychologists that the success of the DDM is overwhelming [25, 26], though in many cases this requires non-trivial modifications or extensions, as time-dependent thresholds [27] or dynamic changes on the drift [28]. Furthermore, recent works have shown that value-based decisions can be also accommodated within

this framework provided that the thresholds are assumed to collapse progressively over time [29, 30].

On the contrary, stochastic mechanisms able to capture the dynamics during sequential decision-making are scarce [31] due to their complexity. Here we will provide experimental evidence that those processes in humans, or at least those of a certain type, are compatible with a stochastic framework in which computational information (through Shannon's entropy) could be implicitly computed by the individual as a way to measure the information gathered. To illustrate this, we study the performance of subjects during a particular navigation task through a maze on the computer screen, combined with eye-tracking data to assess the corresponding behavioral dynamics. We do not introduce any explicit costs for prospecting or analyzing information, as there are no time constraints present in the task. Thus we pose an extreme situation where decisions are mostly driven by optimization of the prospection process, rather than by any speed-accuracy trade-off or any other constraint. This represents an idealized scenario in which the underlying process used by the individuals to reach decisions could be observed without the interference from other factors.

In Section II we will present our information-based framework and discuss its main conceptual differences with accumulator models used for perceptual decision-making. In Section III we will show our experimental results to describe the performance of the subjects in the navigation task. Comparison of those performances to those shown by virtual (random-walk) algorithms able to prospect information ideally, allows us to infer the level of information that humans really process during the task. This reveals that human performances can only be explained if prospection is actually being used in the task, and we can even quantify that level of prospection. Next, we explore the statistical properties of the response time dynamics observed during the task to provide quantitative evidence that humans performances are compatible with the entropy-based mechanism proposed here. The conclusions from these results are then discussed in Section IV, and the experimental and numerical methods employed for the analysis are detailed in Section V.

II. THEORETICAL FRAMEWORK

A relevant problem in decision-making is to establish a criterion to identify when we have enough information to discriminate between alternative options, e.g. options A and B (in a binary case). This can be accounted for by sequential analysis. Let $\mathbf{x}_n = \{x_1, x_2, \dots, x_n\}$ be a set of independent observations that provide some information about the options. We want to use this set to test the hypothesis H_A (corresponding to the option A being valid). Then we need a criterion to determine whether the set \mathbf{x}_n provides either a sufficient level of evidence in favor of (or against) H_A , or a larger set is required and

then additional information must be gathered. The solution to this problem originally developed by Abraham Wald was the well-known Sequential Probability Ratio Test (SPRT), which can be proved to minimize the size n of the set required to accept or reject the hypothesis with a fixed level of reliability [33]. Given the set \mathbf{x}_n , we can map all its information into the joint probabilities $p_{A,n}$ and $p_{B,n}$ (with $p_{A,n} = 1 - p_{B,n}$ if the two options are mutually exclusive) that we assign to options A and B , respectively. The SPRT criterion establishes then from the corresponding cumulative log-likelihood function

$$W_n = \ln \left(\frac{p_{A,n}}{p_{B,n}} \right) \quad (1)$$

that a decision can be reliably taken as soon as W_n exceeds (or falls below) a given threshold (W_{th}). Consequently, the SPRT criterion establishes that there is a minimum amount of evidence required to decide, and actually the DDM can be seen as a particular continuum implementation of it [32, 33].

In controlled experiments of perceptual decision-making, the set \mathbf{x}_n corresponds to direct sensory evidence that can be mapped into the probabilities $p_{A,n}, p_{B,n}$ in a relatively easy manner. For example, \mathbf{x}_n can typically account for visual evidence in favour of one of the two options gathered by the subject during the task. However, in sequential decision-making the existence of such a mapping is far less obvious. Still, some relation between sensory evidence and the internal (mental) assessment of probabilities for options A and B is expected to be carried out by the individual. To simplify, we start by assuming that in sequential-decision making subjects mainly use sensory evidence as a way to estimate the average payoff associated to each option. Following, as above, the binary example for simplicity, we denote such estimated payoffs as $E_{A,n}$ and $E_{B,n}$ after the information in \mathbf{x}_n has been gathered. If we are able to find a criterion to determine how the estimations $E_{A,n}$ and $E_{B,n}$ are carried out, this can be translated into a probability map using the Maximum Entropy Principle (MEP) from information theory. According to the prescriptions from the MEP [34], if the only information available we have from a stochastic variable (an estimation of a payoff, in this case) consists of its average $E_{i,n}$ (with $i = A, B$), then the most neutral (or unbiased) choice of a probability map $p_{i,n} = p_{i,n}(E_{i,n})$ we can build out of it reads

$$p_{i,n} = \frac{e^{\beta E_{i,n}}}{Z_n}, \quad (2)$$

where β is a positive constant (which appears as a Lagrange multiplier when applying the formalism of the MEP) and Z_n a normalization factor that guarantees that $\sum_i p_{i,n} = 1$ holds.

Note that this formalism is equivalent to canonical or Maxwell-Boltzmann statistics in statistical physics (except for a minus sign in the exponential, that can be absorbed in the definition of β). Interestingly, combining

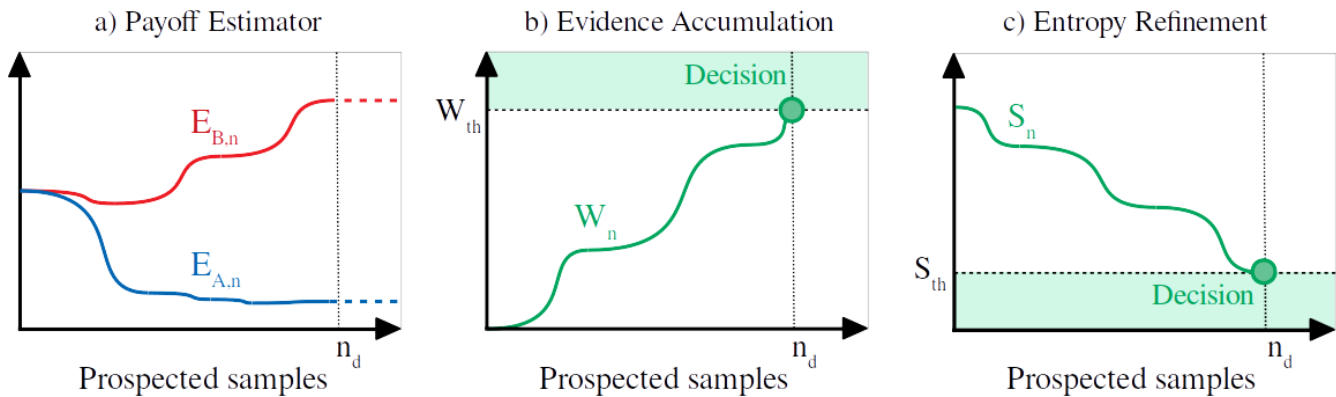


FIG. 1. Scheme for the accumulator and reliability mechanisms. (a) Payoff estimation during successive prospected samples n . (b) Wald's ratio W_n evolution according to the payoff estimators (the decision is taken at n_d when W_n reaches the threshold W_{th}). (c) Shannon's entropy S_n evolution according to the payoff estimators (the decision is taken at n_d when S_n reaches the threshold S_{th}).

(1) and (2) leads to $W_n = \beta(E_{A,n} - E_{B,n})$, so the SPRT can be interpreted in this context as a criterion that imposes a threshold in the difference between the estimated payoffs to take the decision.

In perceptual decisions for which \mathbf{x}_n translates easily into an estimation of probabilities, and time constraints are strong (these are the most typical experimental conditions used), the criterion to minimize the size of the data-set \mathbf{x}_n given by the SPRT represents an adequate solution. However, when time is not a significant constraint and the decision process requires a slow and reflective processing, as in sequential decision-making, then alternative mechanisms should be explored.

Here, we argue that a plausible mechanism for such situations must be based on assessing the amount of information that the probability map (2) contains. The most direct way for computing such information is obviously Shannon's entropy $S_n = -\sum_i p_{i,n} \log(p_{i,n})$ (where again $i = A, B$ for the simplest case of binary decisions). Then, we hypothesize that the easiest way to address sequential decision-making would be to impose a threshold in entropy, S_{th} , such that the condition $S_n < S_{th}$ (with S_n obtained, as explained above, from the evidence available) will trigger the decision in favor of the most likely option at that moment. At this point, we remember that Shannon's entropy reaches its maximum value when no information is still available (so $p_{A,n} = p_{B,n}$), and its value decreases as long as higher evidence in favour of one particular option is gained.

Then, the *evidence accumulation* mechanism typically associated to the SPRT is here replaced by an *entropy refinement* mechanism (see Fig. 1). Actually, we note that this idea is not completely novel but other authors have discussed before similar ideas [35–37], though to our knowledge this specific criterion and its implications have never been tested experimentally.

A. Working example

We will illustrate some specific properties of the *entropic refinement test* (ERT) through an idealized working example. Our main purpose is to detect some relevant (experimentally measurable) differences in the decision-time dynamics that allow us to discriminate between the ERT and the SPRT.

We will focus on the binary decision case again (though we will relax this assumption below). If the individual has to choose between options A and B (whose actual payoffs read μ_A and μ_B , respectively), this will be done by sampling successively information from the two options to obtain estimates $E_{A,n}$, $E_{B,n}$ of the corresponding payoffs (with n again representing the number of steps, or samples). At the i -th step the piece of information obtained by the individual will consist of two Gaussian variables $\epsilon_{A,i}$, $\epsilon_{B,i}$ with corresponding means μ_A , μ_B , respectively, and unit variance. Then, the information obtained provides an approximation to the actual values μ_A , μ_B , and the estimated payoffs can be computed through the average over the information sampled, so $E_{A,n} = \frac{1}{n} \sum_{i=1}^n \epsilon_{A,i}$ and $E_{B,n} = \frac{1}{n} \sum_{i=1}^n \epsilon_{B,i}$. Note that this is in agreement with our assumption above that the individual essentially uses sampling of information to obtain an averaged estimation of the actual payoffs.

Once we have the estimations for the payoffs, we can compute (with the help of (2)) the Shannon's entropy over the information sampled, and explore the decision dynamics if a particular threshold S_{th} is used to trigger the decision. The main magnitude we will explore is, as usual in the field, the statistics of decision times, this is, the number of samples n that the individual requires to reach the entropy threshold. Most works in decision-making experiments focus on the average values of the decision time, or alternatively decision time histograms are fitted to gamma distributions [38, 39]. From that analysis, however, it would be extremely difficult to dis-

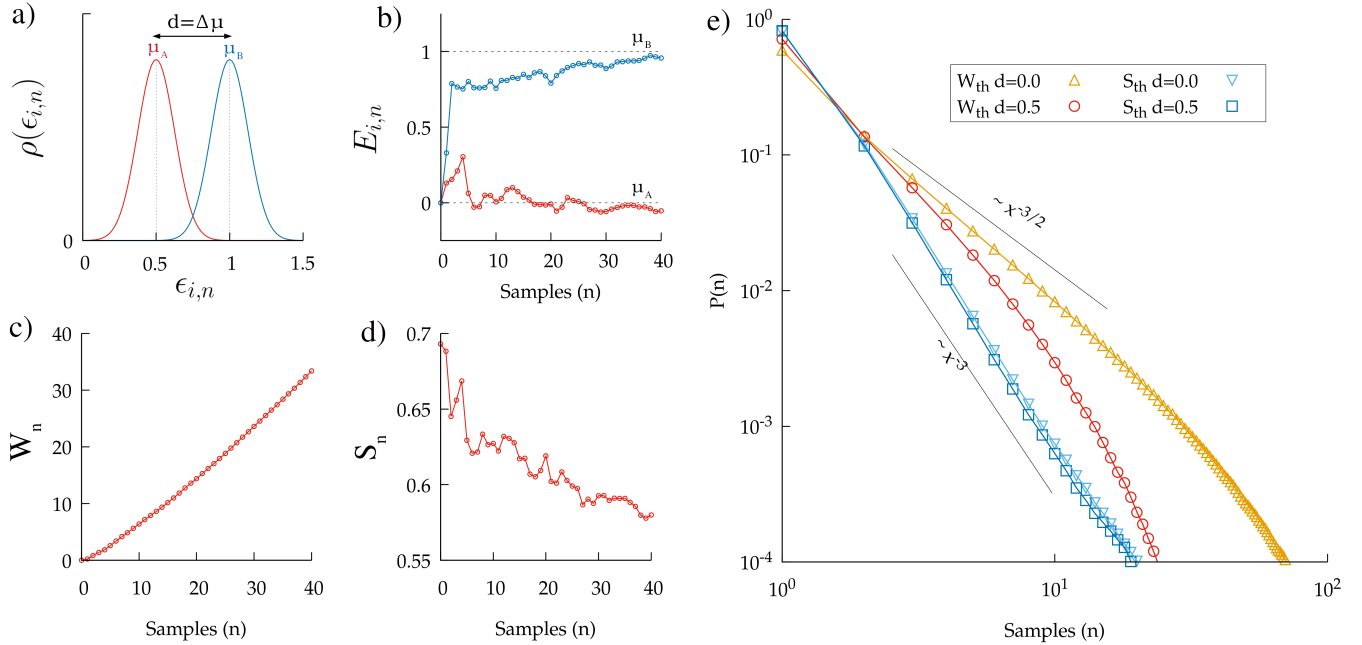


FIG. 2. a) Probability distributions for the stochastic variables $\epsilon_{i,n}$ (with n the number of samples and where i labels the options A and B). The means μ_A , μ_B represent the actual payoffs for each option. b) Evolution of the estimator $E_{i,n}$ as a function of the number of samples n . c) Evolution of the cumulative W_n with the number of samples n . d) Evolution of the Shannon's entropy S_n with the number of samples n . e) Probability distribution for the number of samples to reach S_{th} or W_{th} for the ERT and the SPRT, respectively, and for different distances $d \equiv \mu_B - \mu_A$.

criminate between different decision mechanisms like the ERT and the SPRT, since an appropriate tuning of the parameters could easily lead to similar estimates from both.

Instead, here we will focus on the behavior at the tail of the probability distribution of decision times. Previous works based on ideas similar to the ERT have suggested that this mechanism can account for power-law distributions of decision times [40, 41]. This represents a significant qualitative difference to other mechanisms (as the SPRT) where such distributions often decay in an exponential way.

So that, we carry out numerical experiments using the rules above and determine the distribution of decision times for the ERT and the SPRT, as a function of the parameters μ_A , μ_B , and the thresholds W_{th} , S_{th} (see Fig. 2).

In summary, we find that the SPRT exhibits a time distribution that depends strongly on the distance between the means of the payoffs $d \equiv \mu_B - \mu_A$ (Fig. 2 e)), and for most situations it eventually decays exponentially (though transient power-law behaviors with exponent -1.5 are also found). Instead, for the ERT the distribution exhibits a power law behavior $P(n) \propto n^{-3}$ for a wide range of d and S_{th} values. Remarkably, the power-law behavior with the -3 exponent persists when considering decisions between more than two options; in the Supplementary Material file we show equivalent results for decisions between 4 possible options.

So, at this point we have at least one qualitative difference we can use to discriminate between the SPRT and the ERT.

III. RESULTS

Sequential decision making requires a mental processing of the acquired information which can be hard to capture through monitorization of the brain activity. However, simple situations in which behavioral information reflects somehow such information processing can help inferring the actual mechanisms behind. With this purpose, we have designed a particular navigation task through a maze on the computer screen. Commercial eye-trackers are used during the task to determine where the subjects are gazing at, and from that we obtain information about the possible future paths that the subjects are prospecting at each moment.

The subjects are asked to visit the maximum amount of nodes possible of a discrete 7×7 lattice on the screen within 49 moves if starting from the center of the structure. Moves are only allowed between neighbour nodes, and they are carried out by clicking with the mouse on the node to which one wants to move next. Heterogeneities in the lattice and three different levels of visual complexity (Rectangular, Circular Ordered and Circular Disordered, see left column in Fig. 3) are introduced in order to evaluate the subjects performance under different situations.

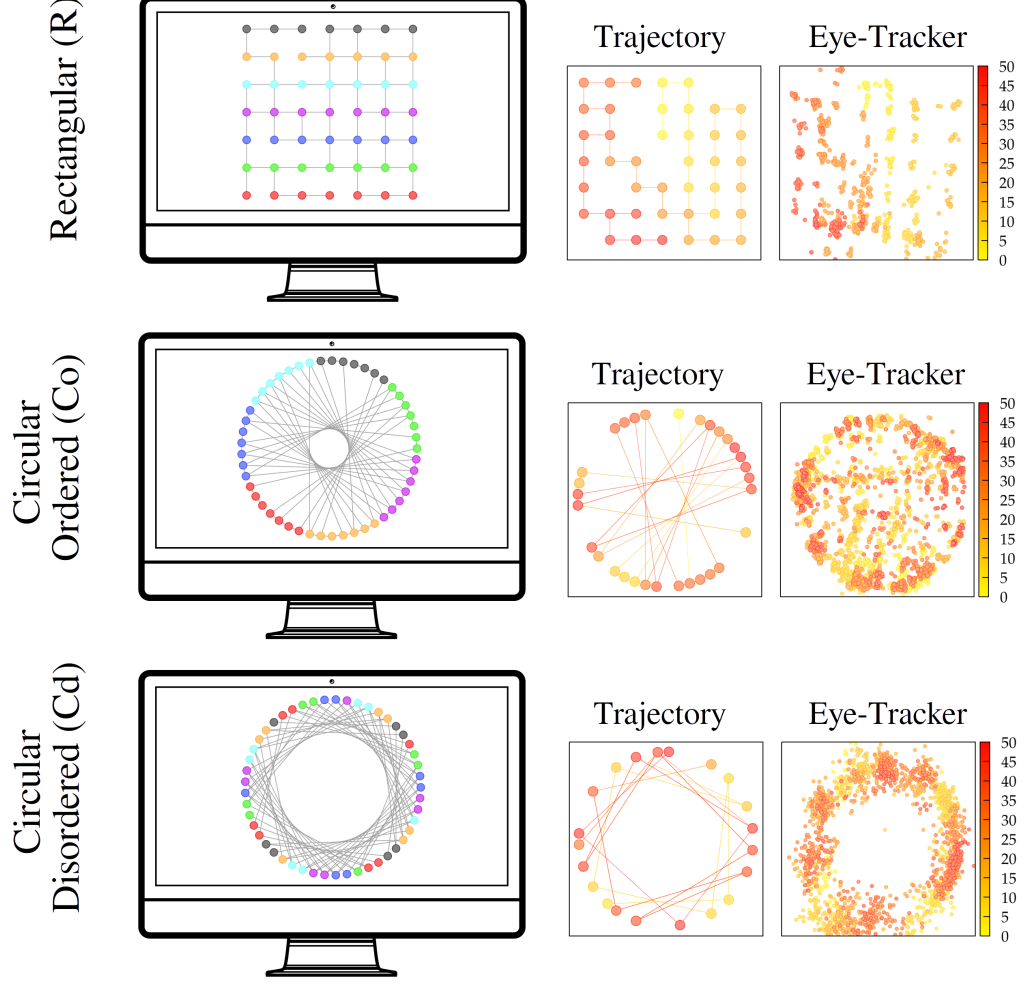


FIG. 3. *Scheme of the experimental setup. First column: Visualization of the 49-node lattice used for the navigation task. The solid lines indicate the bonds allowed between neighbour nodes. Second column: a realization of an individual trajectory within the lattices (the color code denotes time, see legend). Third column: eye fixations obtained during the previous trajectory from eye-tracking data.*

However, all the structures presented to the subjects are topologically identical to facilitate comparison of the results, only visual representation changes from one to another. Further details about the experimental design and protocol are provided below in Section V.

A. Overall performance in the navigation task

The overall performance of the individuals is computed as the number of nodes that have been covered during the entire trajectory of 49 moves (Fig. 4 a)). For the Rectangular level, the subjects visited in average 37.1 ± 3.8 nodes (this is, a 75,7% of the total 49 nodes). For the Circular Ordered level, they covered 29.1 ± 4.8 nodes (59,4%) and for the Circular Disordered graph, 26.4 ± 4.8 nodes (53,9%). These results confirm that the naviga-

tion task (and so the sequential decision making involved) largely depends on the visual representation of the nodes in the lattice, with more complex representations probably preventing the subjects from planning their trajectories ahead (so suppressing prospection). Furthermore, analyzing the performances as a function of the averaged decision time shows us that a higher performance is not a result of spending more time before deciding (Fig. 4 b)), but the difficulty of the task seems to be clearly the driving force explaining those differences (note that the decision time is here defined as the time between consecutive moves).

B. Eye-tracking data capture prospection dynamics

We next analyze the information gathering during the task with the help of the eye-tracking data. We define the distance d_b as the minimum number of moves required to go from the current node of the lattice to the one the individual is gazing at. The corresponding distributions of d_b found are again completely different for the three levels of visual organization (Fig. 4 c)). Then it is clear that the individuals cannot prospect equally in the three cases. While for the Rectangular level a large amount of time is invested in gazing at nearby nodes, for the two Circular levels (specially for the Disordered one) frequent gazes at distant nodes are observed. These must be attributed either to (i) distractions caused by the presence of nodes which are close on the screen configuration though they are not easily accessible from the current one, or (ii) the difficulty at identifying easily the nodes which are available in the next few steps. Ideally, an efficient prospection of the future paths should combine an intensive exploration of closer nodes and a smaller (but non-negligible) exploration of further ones. We illustrate this in the inset of Fig. 4 c), where the cumulative probability of gazing at nearby nodes (defined as those with $d_b \leq 4$) is shown to decrease drastically as a function of the visual difficulty of the task.

C. Quantifying prospection during navigation

As a way to quantify and refine the ideas above, we compare the subjects performance in our task to that of virtual subjects following an algorithm which is able to automatically prospect the information of the paths available within a certain number of moves d_p (called the *prospection length*) in the lattice. While a classical random-walk algorithm would select its path completely at random, making uninformed decisions, our virtual subjects (walkers) have the ability to use the information from the paths prospected to avoid revisits to previous nodes as much as possible, using then a mechanism of self-avoidance. Actually, we follow similar rules to those of the true Self-Avoiding Random Walk [42–44] and the Self-Attracting Random Walk [45–47] schemes to generate the payoffs $E_{j,n}$ (see Section V for details), so then the procedure described in Section II can be applied within the lattice to generate our virtual random walks with prospection.

To enhance its performance, it is then necessary that the virtual walker keeps in memory its previous trajectory. To implement this in a realistic way, we consider that previous visits to a patch are kept in memory by the walker during a characteristic time τ_m . As a result of this finite memory, the corresponding payoffs $E_{i,n}$ will be modified. For large values of τ_m memory remains untouched, and so all visited sites are remembered. On the contrary, for small τ_m previous nodes will be forgotten and so all values of $E_{i,n}$ will be always similar, leading to

a very homogeneous probability map (note that if all $E_{i,n}$ values are the same, according to (2) the same probability will apply to all neighbour nodes, and so the virtual walker will behave in a random, uninformed way).

The rules above allow the virtual random walkers to avoid overlaps in their trajectories. However, their performance, contrary to that of human subjects, is independent of the visual organization of the lattice (Rectangular or Circular). Thus, we can use the comparison between both to assess the prospection abilities that are being presumably used by the human subjects in each level of the experiment.

By exploring a reasonable range of d_p and τ_m values in the algorithm, we observe that the parameter phase space can be divided into four regions (see Fig. 4 d)). For region I the algorithm produces an averaged number of visited nodes lower than the individuals in any of the experiments. The region II produces a performance which lies between the results obtained between Circular Ordered and Circular Disordered. The region III overcomes the results for the Circular Ordered performance but not for the Rectangular. The region IV, finally, outperforms all the experimental results.

Hence, we conclude that relatively large values of both τ_m and d_p are necessary for the virtual walkers to equal or improve the performance by the subjects in the Rectangular level. This seems to confirm that the subjects in this case do actually remember the previously visited nodes during the task, and predict future paths efficiently. The prospection ability, in particular, is indispensable to justify the performances seen in the experiments. Instead, for the Circular structures the individuals are probably not able to prospect the paths to distant nodes (information gathering is less efficient, as suggested before in Fig. 4 c)); in consequence, the value of d_p necessary to reproduce their performance is not necessarily high (though still some level of memory τ_m is necessary).

Next we determine those values of d_p and τ_m that provide the best fit to the distribution of performances obtained from the experiments (see Fig. 4 e)). These are (i) $\tau_m^R = 70$, $d_p^R = 5$, (ii) $\tau_m^{Co} = 7$, $d_p^{Co} = 3$, and (iii) $\tau_m^{Cd} = 5$, $d_p^{Cd} = 2$, for the Rectangular (R), the Circular Ordered (Co) and the Circular Disordered (Cd), respectively.

From this, we analyze the evolution of the performance throughout the task between humans and the virtual walkers with the fitted parameters (Figure 4 f)). The performances increase almost linearly in the beginning, but the growth slows down as the time advances and trajectory overlaps appear in consequence. The experimental curves (symbols) and those obtained from the virtual walkers (lines) agree almost perfectly. This confirms that the behavior of virtual walkers with prospection reproduces in detail the dynamic performance of human subjects throughout the experiment, and so it provides a reliable approximation for it.

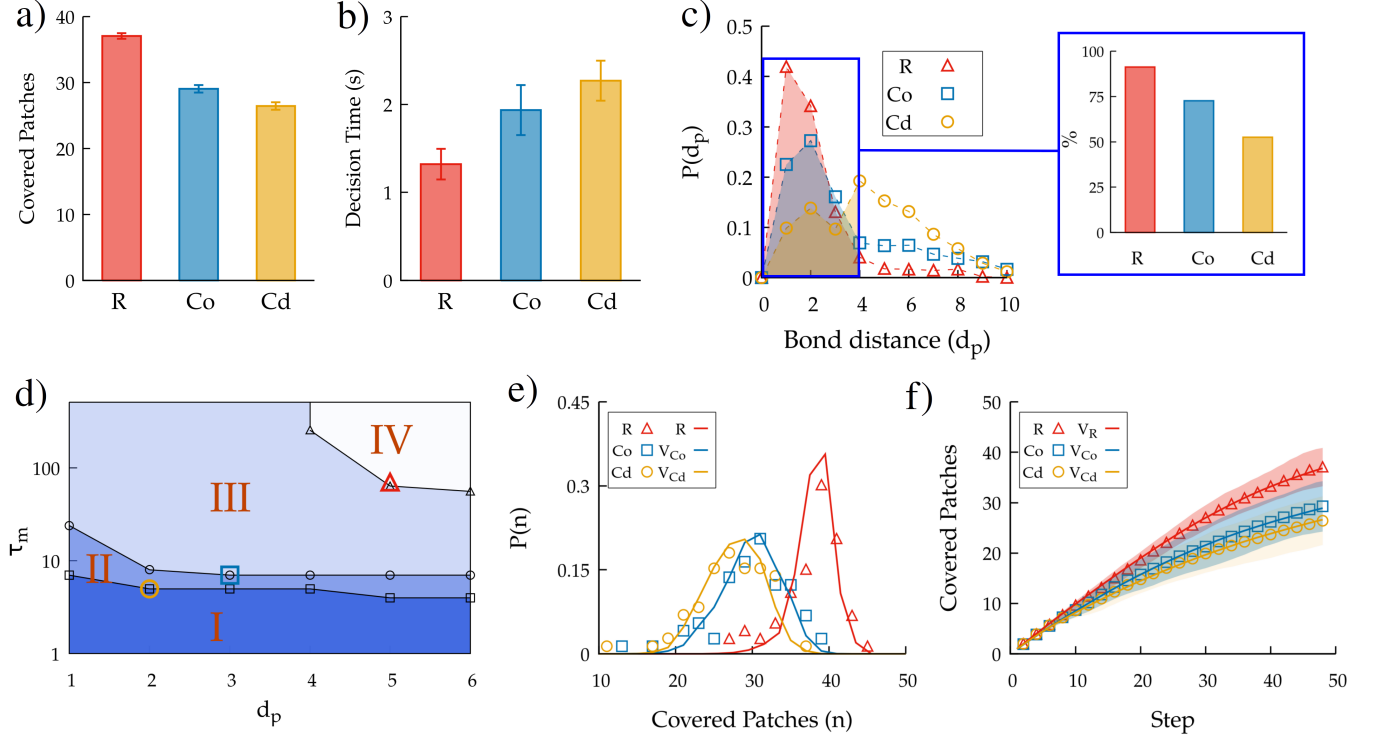


FIG. 4. *a)* Performance of human subjects in the task for the three levels of visual organization presented in Fig. 3. *b)* Averaged decision times for the three levels. *c)* Distribution of the distance d_b between the current node and nodes gazed between moves (Inset: cumulative probability that the nodes gazed satisfy $d_b \leq 4$). *d)* Performance of the virtual walker in comparison with experimental ones, with regions II, III and IV accounting for virtual walker performances better than humans in the R, CO and CD cases, respectively. *e)* Best fit (lines) to the experimental distribution of performances (symbols) obtained from the virtual walker algorithm (see text for details of the fit). *f)* Evolution of the performance during the 49-move trajectories obtained from experimental trajectories (symbols) and virtual walkers with best-fit parameters (lines).

D. Human decisions during maze navigation are compatible with the ERT

The working example explored in Section II yields a power-law scaling (with exponent -3) for the tail of the decision time distributions within the ERT framework. Actually, this result is not specific of that particular example (based on Gaussian estimations of the actual pay-offs). Using the virtual random-walks with prospection described in the previous Section, we obtain exactly the same behavior (Fig. 5 d)) under a wide range of parameter values for d_p , τ_m and S_{th} , so we can infer that this represents a rather general property of the mechanism proposed (see Section V for further details).

To check if the performance of human subjects in the navigation task shows also the same scaling, we use now the eye-tracking data from the experiments to analyse the distributions of *(i)* times between consecutive moves in the experiment, t_m , *(ii)* times during which the subjects gaze at the same patch, t_g , and *(iii)* number of different nodes gazed before making the next move, n_g . The first one would represent our best estimation of the decision times in the experiment, while the other two

are also provided as alternative measures for the sake of completeness.

The results found show a consistent evidence in favor of a power-law scaling with exponent close to -3 for the three cases t_m , t_g and n_g (Figs. 5 a) to 5 c)). Despite the different performances found above (Fig. 4) for the subjects in the three levels of organization (Rectangular, Circular Ordered and Disordered), it is remarkable that they all exhibit extremely similar behavior in this case. This suggests that a common underlying mechanism for decision-making is being used by the subjects in the experiment, though the different difficulty of each leads also to differences in the performances. While the range over which the power-law scaling extends is not very wide (since the decision times in the experiment only span through two orders of magnitude) the fits shown are quite robust. Only longer decision times (for which statistics is not very significant since very few decisions extend so much time) show significant departures from it. Furthermore, we noted in Section II that the classical SPRT often predicts gamma distributions of decision times with exponential decays, so we remark that this classical framework would be completely unable to ex-

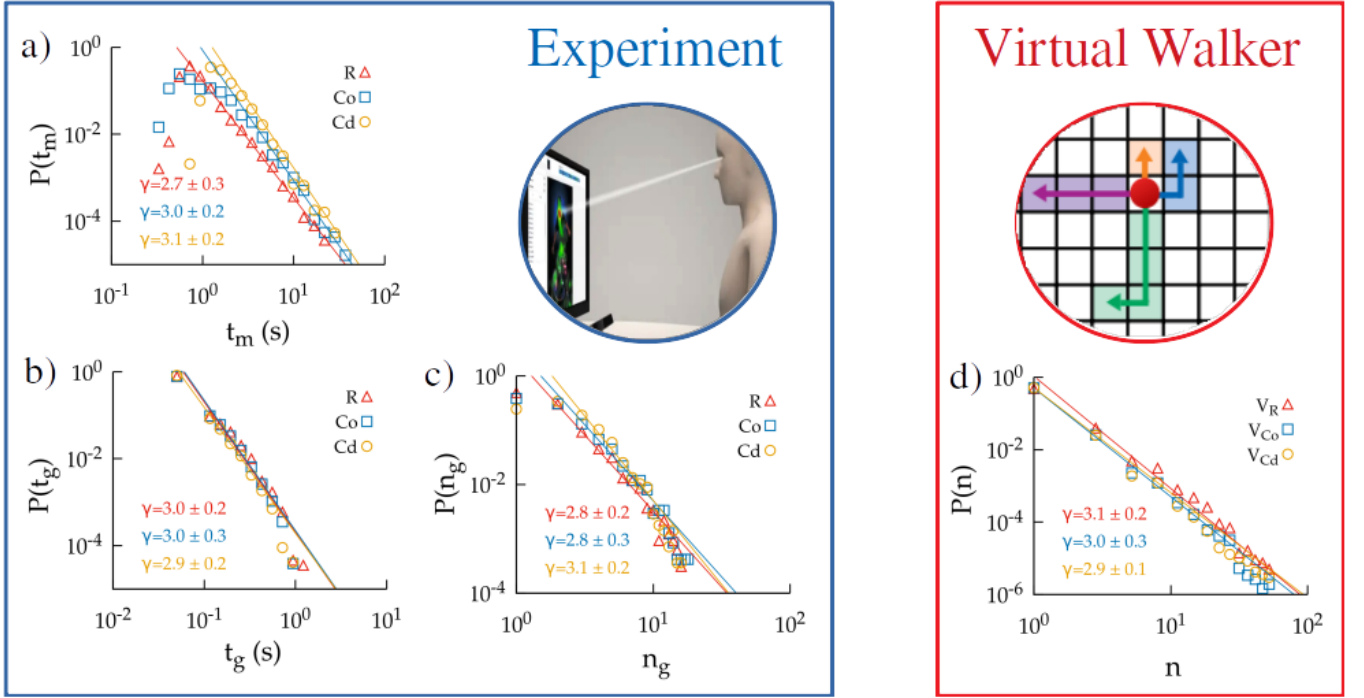


FIG. 5. Distributions for time between consecutive moves t_m (a), the gazing times at a given node t_g (b) and the number of gathered patches between consecutive movements n_g (c) obtained from the experimental data. d) Distribution of the number of prospectings n performed by the virtual random walker. In all cases, the exponent obtained from a power-law fit to the distributions is highlighted, with the different colors representing the difficulty levels R, CO and CD.

plain these results.

E. Information statistics at the moment of the decision

To provide further evidence of the compatibility of the experimental results with the ERT against the SPRT, we explicitly plot the estimated cumulative evidence experimentally obtained by the subjects also at the moment of the decision. Since we cannot now which paths the subject is really prospecting, as a proxy for computing this evidence we compute the fraction of time they have been gazing at regions which are in the same direction that the particular node (see Fig. 6 a)). Starting from the current node, we divide the lattice in four regions, so each eye fixation that lies in a particular region provides further evidence in favour of the corresponding option (A, B, C or D, for the example in Fig. 6 a)).

As mentioned above, the SPRT criterion with canonical probabilities (2) is equivalent to assume that the decision is triggered once the relative evidence reaches a given threshold. Our data clearly shows that the relative evidence estimators computed at the moment of making a decision/move increase monotonically with the time that it has been necessary to take the decision. So, longer decisions involve longer evidence accumulation (figure 6 b)), which is in clear contradiction with the SPRT.

Instead, the ERT proposes that the decision is triggered by a threshold in the informational (Shannon's) entropy S_n . When plotting this entropy (computed from the procedure above) at the moment of the decision, it reaches always a value which is approximately constant (independent of the extent of the decision time), suggesting that this magnitude is really an invariant for all the decisions (Fig. 6 c)). The statistical significance of this result has been verified by testing the null hypothesis that the entropy is non-constant (see figure caption for details). Our conclusion is robust basically for intermediate and longer decisions, while the shorter ones (< 2 seconds) may be probably induced by an automatic response by the subject, or may be based on prior information gathered during the previous move by the subject, so they step away from the decision dynamics above (actually, the -3 power-law scaling discussed above is essentially obtained for decision times in the same range, too).

IV. CONCLUSIONS

Navigation efficiency in higher organisms (humans, in particular) must take into account the fact that they are able to prospect the future outcomes of their available options, and process the corresponding information in order to reach a decision. Here we have explored this idea

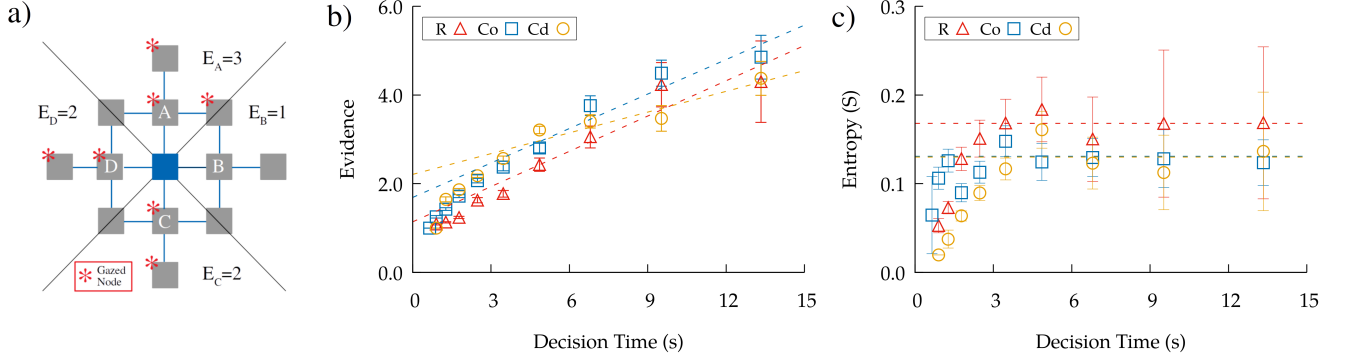


FIG. 6. *a)* Schematic representation of how to estimate evidence from experimental gazes. The asterisks denote eye fixations so all fixations lying in the same quadrant of one option (e.g. option A) provide evidence in favor of that option. *b)* Maximum relative evidence between the options at the moment of the decision. Linear fits (for times larger than 3 s) are given by $f(x) = 0.26x + 1.14$ (R), $g(x) = 0.26x + 1.69$ (CO) and $z(x) = 0.16x + 2.21$ (CD). *c)* Shannon's entropy S_n at the moment of the decision. The horizontal lines correspond to the averaged entropy for times > 3 s (0.168 (R), 0.131 (CO) and 0.130 (CD)). Statistical test for the null hypothesis that the entropy is non-constant for times > 3 s. The corresponding p -values are $p = 0.82$ (R), $p = 0.69$ (CO) and $p = 0.92$ (CD).

within the context of human navigation through mazes when non-local information is available through visual inspection (and so information is processed in a tree-like fashion).

Our analysis (based on comparing the performances of human subjects and those of virtual walkers with the capacity to prospect future paths) provides evidence that prospection is actually being used by the humans, at least in those levels of visual organization that enable it (the Rectangular one, essentially). Besides, an approximate quantitative characterization of that prospection capacity (d_p) and the associated memory skills (τ_m) has been obtained so, reaching an estimation of the quantity of information that humans are really managing during the task.

Furthermore, the distribution of times between moves, or gazing times, together with the study of the values for the entropy at the moment of the decisions allow us to think that the ERT hypothesis proposed here can account to a significant extent for how information is being processed by the subjects during the task. At this respect, we stress that traditionally mean times to decision, as well as the ratio of the times corresponding to choosing option A or B (for binary decisions) have been studied in detail by psychologists. On the contrary, the tails of the decision time distributions are rarely explored decision-making experiments. In contrast, here we have shown that this statistical analysis provides very significant information about the dynamics of decision that is being used in the experiment (and actually non-exponential decays in those distributions clearly seem to indicate that the classical SPRT can hardly be used to explain this kind of tasks/experiments).

Regarding the -3 value of the power-law exponent we have recurrently obtained from the ERT formalism and from experiments, a formal justification of its origin re-

mains unknown for the moment. For the specific navigation task proposed here, note that decision times should be understood as the sum of the times that the individual has been gazing at each node before making a new move. Then, to explain the power-law scaling found for decision times one should argue that either (i) the distribution of times the subject keeps looking at a given patch, or (ii) the number of patches that are gazed between decisions, must have power-law tails. It is, however, the case (Fig. 5 a) and 5 b)) that both distributions present that scaling. So, the underlying mechanism yielding the power-law distribution for decision times is apparently a non-trivial combination of both. It is not still clear yet how general these results may be, or if they appear as a consequence of the conditions used in our experiment in particular. However, we stress that similar results have also been found in other experiments of human navigation through mazes [48], so all together raises the need for a deeper and systematic exploration of these ideas in the future.

Finally, it is remarkable that all this information about sequential decision-making in humans has been reached simply with the help of eye-tracking data and monitoring of the decision times exhibited by the subjects on the computer screen, which require just easily available technologies. It is likely that the combination of such methods and data with EEG or other advanced physiological sensors could be used to refine our ideas, and provide more reliable estimates of the dynamics during similar tasks, also in more realistic environments than the one here. We expect that our results can stimulate further research in this line.

V. METHODS

A. Experimental Design

18 clinically normal adults (10 women and 8 men) aged from 18 to 45 carried out the experiment. In the first part of the task, subjects are presented a discrete 7x7 regular lattice on the screen (Fig 3, upper panel on the left). The patches are linked through bonds connecting them only to neighbour patches (4 paths per node, except for the boundaries where paths are only 2 or 3). However, we remove a part of the bonds between nodes (20% of them, always preventing isolated regions in the structure from being formed) in order to introduce some level of heterogeneity in the lattice (Fig 3, left column), and then nodes are reorganized in different configurations (Rectangular, Circular Ordered, and Circular Disordered, as mentioned above).

The subjects are asked to visit the maximum amount of patches of the resulting lattice within 49 moves if starting from the center of the structure (one step is defined as a transition between connected nodes in the graph). They are not required to complete the trajectory in any given time, so time constraints are not present in the task and information processing can be extended as much as desired by the subject. They can move to neighbour nodes in the lattice by clicking with the mouse over the patch to which they want to move next (Fig 3, middle columns, show some realizations of the resulting trajectories). Heterogeneity in the lattice then makes the process non-trivial (for a homogeneous regular lattice the optimal strategy would be simply to perform a ladder-like trajectory until covering all nodes).

To facilitate visualization of the options available at each decision (especially in the Circular Disordered case, where visualization could be tough), the current node of the individual was depicted in a different color (green, with the rest of the nodes appearing in blue) and the possible moves available at each moment were emphasized (with thicker solid lines). On the contrary, the subjects have no visual guides to distinguish between previously visited and non-visited patches, so they can only use their memory skills to avoid overlaps and increase their performance.

To assess the subjects performance under different levels of difficulty, the nodes in the Rectangular lattice are then visually reorganized in a circular way. In one case (Circular Ordered), we keep in the circle the order of the rows of the first rectangular graph (Fig. 3 middle row). For the other (Circular Disordered), we place the nodes following a circular structure but with random reorganization of nodes (Fig. 3 lower row). We remark that topologically the three structures are completely equivalent, while visually different. Additionally, we rotated 90°, 180° and 270° the rectangular structure (with their corresponding Circular Ordered and Circular Disordered reorganizations) for randomizing the task (so 12 cases in total, all with the same topological structure, are pre-

sented to each subject). The final data-set comprised then 216 trajectories with a mean duration of 77.1 ± 2.9 s each.

As a proxy for information prospection during the task, we use eye fixations measured through a commercial eye-tracker (Tobii X2-30, at 30 Hz). An eye fixation corresponds to the visual gaze on a single location within the screen. See the right column in Figure 3 for a visual trajectory example for each structure. We use this to analyze (i) the number of nodes at which the subject gazes between consecutive steps, and (ii) the time it remains gazing at particular patches. For this, each node was assumed to be represented by a circle of radius 0.05 (the screen size is equal to 1) around the center of the node, so all eye fixations lying within the circle are assumed to indicate that the subject is gazing at that particular node. This circle size prevents to assign the subject fixations to different nodes at the same time.

B. Virtual walkers with prospection

An algorithm for generating virtual random walks with prospection over the 7x7 lattice used in the experiment is proposed as a reference model against which to compare experimental data. Our virtual walkers are able to estimate the convenience of moving to a neighbour node j by assigning successive values $\epsilon_{j,1}, \epsilon_{j,2}, \dots$ to that node by prospecting hypothetical paths that would use that node as a starting point. So that, at each time step the walker prospects one particular path (chosen at random from all the possible ones) of fixed length d_p (*prospection length*) starting from each of the neighbour nodes. The specific value $\epsilon_{j,n}$ assigned to the n -th prospected path for the neighbour node j corresponds to the fraction of non-visited nodes that the path will cover, with $\epsilon_{j,n} = 1$ representing a prospected path for which all sites are still unvisited, and $\epsilon_{j,n} = 0$ representing a path for which all nodes have been already visited before. So that, the corresponding payoff associated to that neighbour node j (after n paths have been prospected) reads $E_{j,n} = \frac{1}{n} \sum_{i=1}^n \epsilon_{j,i}$, in analogy with the working example discussed above.

Once payoffs have been defined, the procedure described in Section II can then be applied within the lattice to generate our virtual random walks. After each single prospection of one path in each direction, the walker computes the corresponding Shannon's entropy $S_n = -\sum_i p_{j,i} \ln p_{j,i}$; if the computed value falls below a fixed threshold S_{th} , the walker makes the decision (it is, a move) according to the probabilities $p_{j,i}$ computed (we have checked that choosing instead the node with the highest probability leads to very similar results). On the contrary, if $S_n > S_{th}$ then the prospection process continues. However, at practice we introduce a rule such that the maximum number of prospectations is limited to 100 to avoid (extremely unusual) situations in which S_n would never decay below S_{th} because all options persistently ex-

hibit very similar payoffs (this rule doesn't significantly modify any of the results reported here).

Distributed prospection lengths. Assigning a constant prospection length d_p to all the prospected paths may seem rather unrealistic. Human subjects are expected instead to prospect paths with different lengths depending on the specific situation (complexity, number of choices available, etc). The results in Fig. 5 b) also support this, as the number of gazed patches exhibits a variation which spans almost one order of magnitude.

We have studied then our virtual random-walk algorithm for the case when a distribution of d_p is introduced instead of a constant value. We have tried in particular a distribution $P(d_p) \propto \frac{1}{d_p^\gamma}$ (for $d_p \geq 1$ and with γ going from 0 to ∞), with $\sum_{d_p=1}^{\infty} P(d_p) = 1$ to guarantee normalization. The results, which are summarized in the Supplementary Material File, clearly show that the conclusions one obtains so are qualitatively the same as those presented for fixed d_p values in the main text.

Robustness of the distribution of decision times on the entropy threshold S_{th} . We have reported

above that the decision time for the walker exhibits the power-law distribution with exponent -3 . An analysis to check that this exponent remains approximately constant, independently of the memory and prospection parameters d_p and τ_m , as well as the threshold S_{th} , has been carried out using our virtual random-walk algorithm. According to the results found (see the Supplementary Material file), the conclusions reached in the article remain quite robust. Only when very large or very small values of S_{th} are considered (which would represent the case in which decisions are either taken almost immediately without barely any information gathering, or an extremely large amount of information would be necessary to trigger the decision) the $\sim n^{-3}$ scaling breaks down.

VI. ACKNOWLEDGEMENTS

This research was supported by the Spanish government through Grant No. CGL2016-78156-C2-2-R.

-
- [1] J. I. Gold and M. N. Shadlen. *The Neural Basis of Decision Making*. Ann. Rev. of Neuroscience, 30 535-574 (2007).
 - [2] S. P. Kelly and R. G.O'Connell. *The neural processes underlying perceptual decision making in humans: Recent progress and future directions*. Journal of Phys.P 109, 27-37 (2015)
 - [3] S. Blakemore and T. W Robbins. *Decision-making in the adolescent brain*. Nat. Neurosci. 15 (2012)
 - [4] B. De Martino, D. Kumaran, B. Seymour and R. J. Dolan. *Frames, Biases, and Rational Decision-Making in the Human Brain*. Science 313, 684-687 (2006)
 - [5] D. Lee. *Game theory and neural basis of social decision making*. Nat Neurosci. 11, 404-409 (2008)
 - [6] D. Lee, M. L.Conroy, B. P.McGreevy and D. J.Barraclough. *Reinforcement learning and decision making in monkeys during a competitive game* Cognitive Brain Research 22, 45-58 (2004)
 - [7] I. Couzin, J. Krause, N. Franks and S. A. Levin. *Effective leadership and decision-making in animal groups on the move*. Nature 433, 513-516 (2005)
 - [8] A. J. W. Ward, D. J. T. Sumpter, I. D. Couzin, P. J. B. Hart and J. Krause. *Quorum decision-making facilitates information transfer in fish shoals*. PNAS 105,19) 6948-6953 (2008)
 - [9] G. Valentini, E. Ferrante and M. Dorigo. *The Best-of-n Problem in Robot Swarms: Formalization, State of the Art, and Novel Perspectives*. Front. Robot. (2017)
 - [10] L. Conradt and C. List *Group decisions in humans and animals: a survey*. Phil. Trans. R. Soc. B 364,1518 719-742. (2009)
 - [11] S. Redner. *Reality-inspired voter models: A mini-review*. Comp. Rend. Phys. 20, 4 275-292 (2019).
 - [12] P.A. Ortega and D.A. Braun. *Thermodynamics as a theory of decision-making with information-processing costs*. Proc. R. Soc. A 469: 20120683 (2013).
 - [13] V.I. Yukalov and D. Sornette. *Self-organization in Complex Systems as Decision Making*. Adv. Complex. Syst. 17, 1450016 (2014).
 - [14] P. Schwartenbeck, T. FitzGerald, R.J. Dolan and K. Friston. *Exploration, novelty, surprise, and free energy minimization*. Front. Psychol. 7:2013.00710 (2013).
 - [15] É. Roldán, I. Neri, M. Dörpinghaus, H. Meyr and F. Jülicher. *Decision Making in the Arrow of Time*. Phys. Rev. Lett. 115, 250602 (2015).
 - [16] M. Favre, A. Wittwer, H.R. Heinemann, V.I. Yukalov and D. Sornette. *Quantum Decision Theory in Simple Risky Choices*. PLoS ONE 11:e0168045.
 - [17] K. H .Britten, M. N. Shadlen, W. T. Newsome and J. A. Movshon *The analysis of visual motion: a comparison of neuronal and psychophysical performance*. J Neurosci 12,12 (1992)
 - [18] J. D Roitman 1 and M. N Shadlen *Response of neurons in the lateral intraparietal area during a combined visual discrimination reaction time task* . J Neurosci. 22,21 (2002)
 - [19] E.M. Tartaglia, A.M. Clarke1 and M.H. Herzog. *What to Choose Next? A Paradigm for Testing Human Sequential Decision Making*. Front. Psychol. 8:312 (2017).
 - [20] D. Zhang and R. Gu. *Behavioral preference in sequential decision-making and its association with anxiety*. Hum. Brain Mapp. 39:2482-2499 (2018).
 - [21] D.T. Gilbert and T.D. Wilson. *Prospection: Experiencing the future*. Science 317, 1351-1354 (2007).
 - [22] T. Suddendorf and M.C. Corballis. *The evolution of foresight: What is mental time travel, and is it unique to humans?*. Behav. Brain Sci. 30, 299 (2007).
 - [23] B.E. Pfeiffer and D.J. Foster. *Hippocampal place-cell sequences depict future paths to remembered goals*. Nature 497, 74-81 (2013).
 - [24] R. Ratcliff, P. L. Smith, S. D.Brown and G. McKoon *Diffusion Decision Model: Current Issues and History*. Trends in Cog. Science, 20 260-281 (2016).

- [25] R. Ratcliff and G. McKoon. *The Diffusion Decision Model: Theory and Data for Two-Choice Decision Tasks*. Neural Comput. 20 873–922 (2008).
- [26] A. Rangel et al. *The Drift Diffusion Model can account for the accuracy and reaction time of value-based choices under high and low time pressure*. Judgment and Decision Making, 5 437–449 (2010)
- [27] M. L. Pedersen, M. J. Frank and G. Biele. *The drift diffusion model as the choice rule in reinforcement learning*. Psychon Bull Rev 24 1234–1251 (2017)
- [28] L. Fontanesi, S. Gluth, and M. S. Spektor. *A reinforcement learning diffusion decision model for value-based decisions*. Psychon Bull Rev 26 1099–1121 (2019)
- [29] A. Roxin. *Drift–diffusion models for multiple-alternative forced-choice decision making*. Jou. of Math. Neuroscience 9, 5 (2019)
- [30] S. Tajima, J. Drugowitsch and A. Pouget. *Optimal policy for value-based decision-making*. Nat. Comm. 7:12400 (2016)
- [31] K.P. Nguyen, K. Josić and Z.P. Kilpatrick. *Optimizing sequential decisions in the drift-diffusion model*. J. Math. Psychol. 88, 32–47 (2019).
- [32] R. Bogacz, E. Brown, J. Moehlis, P. Holmes and J.D. Cohen. *The physics of optimal decision making: a formal analysis of models of performance in two-alternative forced-choice tasks*. Psychol. Rev. 113(4), 700 (2006).
- [33] A. Wald and J. Wolfowitz. *Optimum character of the sequential probability ratio test*. Ann. Math. Stat. 32,6–339 (1948).
- [34] E.T. Jaynes. *Information Theory and Statistical Mechanics I*. Phys. Rev. 106, 620–630 (1957).
- [35] G. Collell and J. Fauquet. *Brain activity and cognition: a connection from thermodynamics and information theory*. Frontiers in Psychology 6, 818 (2015)
- [36] K. Friston, J. Kilner and L. Harrison. *A free energy principle for the brain*. Journal of Physiology-Paris, 100 1 (2006)
- [37] D. F. Slezak, M. Sigman and G. A. Cecchi. *An entropic barriers diffusion theory of decision-making in multiple alternative tasks*. PLOS Computational Biology 14(3): e1005961 (2018)
- [38] W. J. McGill and J. Gibbon. *The general-gamma distribution and reaction times*. Journal of Math. Psy., 2 1, 1–18 (1965)
- [39] E. M. Palmer, T.S. Horowitz, A. Torralba and J. M. Wolfe. *What are the shapes of response time distributions in visual search?* J. Exp. Psychol. Hum. Percept. Perform., 37 1, 58–71 (2011)
- [40] J.M. Medina, J. A. Díaz and K. H. Norwich. *A theory of power laws in human reaction times: insights from an information-processing approach*. Front Hum Neurosci., 8 621 (2014)
- [41] J.M. Medina and J. A. Díaz. *Commentary: Piéron’s law is not just an artifact of the response mechanism*. Frontiers in Physiology, 6 190 (2015)
- [42] D. J. Amit, G. Parisi and L. Peliti. *Asymptotic behavior of the “true” self-avoiding walk*. Phys. Rev. B, 27 3, 1635–1645 (1983)
- [43] R. Rammal, J. C. Angles d’Auriac and A. Benott. *Statistics of the true self-avoiding walk in one dimension*. Journal of Physics A, 17 1, 9–14 (1984)
- [44] F. Family and M. Daoud. *Experimental realization of true self-avoiding walks*. Phys. Rev. B, 97 3, 1506–1507 (1984)
- [45] Zhi-Jie Tan, Xian-Wu Zou, Wei Zhang and Zhun-Zhi Jin. *“True” self-attracting walk*. Physics Letters A, 289 4, 251–254 (2001)
- [46] V. B. Sapozhnikov. *Self-attracting walk with $\nu < 1/2$* . Journal of Physics A, 27 6, 151–153 (1994)
- [47] A. Ordemann, E. Tomer, G. Berkolaiko, S. Havlin and A. Bunde. *Structural properties of self-attracting walks*. Phys. Rev. E, 64 4 (2001)
- [48] F.M. Del Prado Martin. *Scale-Invariance of Human Latencies*. Proceedings of the Annual Meeting of the Cognitive Science Society, 31 (2009)